Full Text View

Volume 28, Issue 4 (April 1998)

Journal of Physical Oceanography
Article: pp. 659–668 | Abstract | PDF (192K)

Decadal Wind Forcing of the North Atlantic Subtropical Gyre

W. Sturges, B. G. Hong, and Allan J. Clarke

Department of Oceanography, The Florida State University, Tallahassee, Florida

(Manuscript received April 12, 1996, in final form July 21, 1997)

DOI: 10.1175/1520-0485(1998)028<0659:DWFOTN>2.0.CO;2

ABSTRACT

In the central North Atlantic Ocean there are large decadal-scale fluctuations of sea level and of the depth of the thermocline. This variability can be explained by low-frequency Rossby waves forced by wind. The authors have used a simple model of ocean fluctuations driven by the COADS wind-stress curl and find that their model results and hydrographic data, to the limited extent they can be compared meaningfully, agree rather well.

The variation in wind curl over the ocean leads to surprisingly large north–south variability in the computed oceanic response over the subtropical gyre. The peak-to-peak sea level differences are as great as 20 cm and persist for many years. These large variations could induce major errors in calculations of the mean ocean flow when hydrographic sections from many years are combined. It appears possible, however, to correct for these wind-induced effects to allow the lower-frequency signals to be determined.

The westernmost edge of our oceanic calculations is at the offshore side of the Gulf Stream. These fluctuations show changes in the north–south slope of sea level that imply long intervals of transport into or out of the Gulf Stream and provide suggestive evidence for low-frequency variability in coastal sea level and in the transport of the stream. This variability has been found previously in more complex ocean models, but the simplicity of these calculations may make the forcing mechanism and the ocean's response easier to understand.

Table of Contents:

1. Introduction

This paper is about low-frequency fluctuations in sea level and the thermocline in the North Atlantic subtropical gyre. The work grew out of a program that is focused on variability in the large-scale rise of sea level. The work breaks naturally into two parts: the open ocean response and the coastal response. This paper deals with the results in the open ocean; sea level at the coast is treated in a separate paper.

The rise of sea level and its variability along midlatitude coasts is well known, and we wish to use coastal tide gauge information to help understand the similar fluctuations in the open ocean. In the central North Atlantic, at the latitudes of the subtropical gyre, there is but one island tide gauge: Bermuda. Along the U.S. coast of course, there is a wealth of tide gauge data. The general features are a gradual rise of sea level, which is not in question, embedded in a background of low-frequency variability, which we seek to understand: see, for example, the papers of Barnett (1984), Douglas (1992), Woodworth (1990), and Wunsch (1992). Figures showing these features in sea-level data have been available for a long time (e.g., Hicks et al. 1983); the western edge of the Pacific has fluctuations that are quite similar: see, for example, Barnett (1984) and Douglas (1992).

Sea level at midocean tide gauges, such as Bermuda, shows variability much like that on the U.S. east coast: low-frequency variations having peak-to-peak amplitudes over 10 cm. The record at Charleston is longer; Fig. 1 contains two periodograms of monthly sea level data, from the first and the last 30 years of sea level at Charleston.[1] Results from most U.S. eastern coastal gauges are similar. The stations that have the longest records usually show the long-term sea level rise most clearly. Fluctuations of order 10 cm peak-to-peak are typical of the decadal sea level variability. And this variability, of course, obscures changes in the underlying trend.

We show the spectrum in Fig. 1 with so little smoothing for two reasons. First, at periods shorter than several hundred months, the spectrum falls off approximately as f^{-1}. This feature is evident with almost any amount of smoothing. Second, the two spectra from these pieces of record show peaks at different frequencies, a result that would be expected from essentially random forcing. The difference in power ranges from a factor of 2.5 up to an order of magnitude in different frequency bands; it is reasonable to assume that similar changes exist in the ocean. Though these spectra are not *strongly* red, most such records show that power continues to increase at long periods. That we do not know how steep the spectra really are at longer periods should be a cause for concern. Smoothing the spectra by any reasonable amount causes a loss of the lowest-frequency points, obscuring the fact that the spectrum is red out to these very long periods.

Whether the *rate* of sea level rise is *increasing* is an important question (but not dealt with here). Because power continues to increase at the unresolved low frequencies in Fig. 1, it is apparent that the background rate of sea level rise is difficult to estimate and will depend crucially on the time interval selected (Douglas 1992; Woodworth 1990). In the face of this large variability and with our present records, reliable estimates of *changes* in the rate of rise are quite difficult. Therefore, a major motivation for this work is a desire to understand the fundamental causes of the decadal-scale fluctuations so that they can be rationally removed from the original records in order to expose any changes in the rate of rise.

What causes these large fluctuations? We show here that long Rossby waves, propagating across the Atlantic and forced by open-ocean wind curl, produce large fluctuations in sea level in the open ocean and on the offshore side of the Gulf Stream. The amplitudes and periods of these oceanic fluctuations *suggest* that they are related to the coastal variability. We suggest that the work reported here is an important first step in determining the causes of decadal sea level fluctuations on eastern continental boundaries and, as an added bonus, moves us toward reducing the effects of these large fluctuations in hydrographic observations. The likelihood that wind fluctuations are a major forcing mechanism was suggested to some extent by Maul and Hanson (1991), who found coherence between coastal sea level and atmospheric pressure fluctuations.

Attempts to extract the lower frequency (sometimes called "mean") flow of the open ocean from a collection of historical hydrographic data must correct for these fluctuations in order to obtain meaningful results. We present here calculations that address questions of which time intervals contain large enough departures from the mean that such corrections should be performed in order to suppress (to first order) the time-dependent effects.

Here we have used a simple model in an attempt to isolate the important physical mechanism(s). Other more complex models also can give similar information about sea level. For example, Ezer et al. (1995) and Greatbatch et al. (1991) have used the Princeton Ocean Model and found large decadal-scale changes in sea level that are in agreement with observations.

2. Methods

a. A model of wind forcing over the ocean

The straightforward model of wind forcing used here is patterned after Meyers (1979) and Kessler (1990) and was used by Sturges and Hong (1995). We concentrate on forcing at periods longer than a few years, at which the response will be primarily from long, nondispersive, baroclinic Rossby waves. Price and Magaard (1986)found that waves at these long periods traveled within a few degrees of due westward. Krauss and Wuebber (1982) concluded that first-mode Rossby waves would travel nearly westward at the annual period. Our interest is in periods substantially longer. The results of Liu (1993) suggest that even at decadal scales there may be a significant amount of N–S wave propagation. However, as Mayer and Weisberg (1993) show, the distribution of observed wind forcing is much more limited meridionally than Liu assumed; the region of strongest forcing here in the Atlantic extends only to 36° or 38°N. Because the forcing weakens at higher latitudes, it is unlikely to affect the region of our interest. For these reasons we conclude that at these frequencies a model in which only westward propagation occurs is a useful approximation.

After separation of the linearized equations for a stratified ocean into vertical modes, one finds that the low-frequency, large-scale wind-driven response for pressure for the *n*th mode is described by the product $p_n(x, y, t)F_n(z)$, with p_n satisfying the equation

$$\frac{\partial p_n}{\partial t} - \gamma_n \frac{\partial p_n}{\partial x} = B_n \,\mathrm{curl}(\tau/\rho_0 f), \qquad (1)$$

where p is pressure, t is time, x is the distance eastward, y northward, and z upward; τ is wind stress, f is the Coriolis parameter, ρ_0 is a constant representative water density, $F_n(z)$ is the *n*th vertical mode eigenfunction, and γ_n is the long Rossby wave speed for the *n*th vertical mode:

$$\gamma_n = \frac{\beta c_n^2}{f^2} \qquad (2a)$$

and

$$B_n = -\frac{c_n^2}{f^2}\int_{-H_{\mathrm{mix}}}^{0} F_n\,dz \Big/ H_{\mathrm{mix}}\int_{-H}^{0} F_n^2\,dz. \qquad (2b)$$

In (2) β is the northward gradient of f, c_n is the *n*th vertical mode long gravity wave speed, H is the total depth of the ocean, and H_{mix} is the depth of the surface mixed layer, taken somewhat arbitrarily to be 100 m.

For each mode we calculated the long gravity wave speeds c_n as in Sturges and Hong (1995), in 4° rectangles, from the recent CD-ROM atlas of hydrographic data from the National Oceanographic Data Center. Our speeds are based on data in the individual 4° rectangles, not on data that have been smoothed with a large spatial filter. The resulting wave speeds vary slowly with longitude, in keeping with the observed distributions of density and depth. The wave speeds are calculated a priori and are not tuned for an optimum fit in the results. We found earlier at Bermuda that the model results were not improved by adding vertical modes higher than the first. Here, however, at lower latitudes we find that the addition of the second mode improves the results, beginning at ~ 24°N, and is a substantial improvement at 18°N. It may be worth emphasizing that at these speeds the free modes require many *years* to travel across the Atlantic. Before any output from the model is used, of course, the model is run long enough for the waves to travel across the ocean. One experiment was done in which the model state at the end of a run was used as the initial condition; there was no change in the results. This lack of effect may be caused by the fact that the mean curl is removed from this model; it is driven only by the fluctuations.

The basic question of whether waves of such slow speeds are affected by horizontal advection is not dealt with here. In the earlier work (Sturges and Hong 1995), however, very good results were obtained at 32°N when advection was ignored. Perhaps this should not be surprising, in view of the Chang and Philander (1989) results and in consideration of the finding that our results are dominated by the first vertical mode.

One of our concerns was the choice of depth in the region of irregular bathymetry near the Mid-Atlantic Ridge. We therefore used the depth to which the available mean density data extended in that region. A selection of the resulting wave speeds is shown in Fig. 2; the effect of the Mid-Atlantic Ridge is apparent in the local minima. Picaut and Sombardier (1993) have shown that for the first few modes it is more important to give an accurate specification of stratification than of depth; we have tried to specify stratification carefully.

We used a box size of 4° in latitude and longitude for computing curl as an attempt to reduce the noise of the 2° wind data, yet retain reasonable resolution. Therefore, we also used 4° boxes for computing the speed of Rossby waves to keep the ocean resolution compatible with that of the wind forcing.

Chelton and Schlax (1996) and others have found that at periods near 12 months the observed Rossby wave signals in the TOPEX results travel as much as 50% faster than the free wave speeds would suggest. In our results the waves are partly free and partly forced, but we find, by comparing the effective speeds of the waves with the calculated speeds, that the waves *in our model results* travel only ~ 5% faster than the free wave speeds. To the best of our ability to compare them, our results agree with observations at *these frequencies*. We conclude, therefore, that the effect of direct wind forcing does not substantially increase the observed wave speeds in the frequency band we have studied. We return to this subject in a later section.

b. Structure of wind forcing

It is not clear a priori what horizontal scales in the wind field are necessary for forcing a model for these processes. To explore this question, Fig. 3 shows the average wavenumber spectra for both the east–west and north–south wind curl variability. Although we use 2° resolution in the data for these calculations, recall that we have integrated the wind stress around 4° boxes to compute the curl, so there will be almost no power near the Nyquist wavenumber. The spectral decay from the longest wavenumbers is approximately f^{-2} out to the shortest wavenumbers that are well resolved here, so we have used forcing at the highest resolution available to us. (Recall that the wind averaging in 4° boxes was considered necessary to suppress noise at the smallest scales.) The COADS data are described by Slutz et al. (1985)

One result in Fig. 3 seems worth pointing out. In the north–south direction, as we would expect, the power peak is determined primarily by the size of the wind system over the subtropical ocean. In the east–west direction, however, the power peak is determined essentially by the width of the ocean, not by the structure of the wind system.

Figure 4 shows the distribution of power in the north–south wavenumbers as a function of longitude. For this figure we averaged the power at the two longest wavenumbers (as in Fig. 3); there is an abrupt rise in power in the middle of the ocean. We expect the waves to travel to the west and for the energy to accumulate toward the west; this variation in power (assuming that it is not an artifact of the sampling) makes it even more likely that we should expect to see the largest response in the ocean on the western side. As we shall see later, there is yet another reason why there is a maximum in the west—at these frequencies. The distribution of power in the east–west wavenumbers, by contrast (not shown), shows a simple rise from south to north, peaking around 38°N.

c. Model results in midocean

Figure 5 shows examples of model results along 34° and 18°N; panels (a) and (b) show model output at two latitudes, while (c) and (d) show the wind forcing at those same latitudes. This discussion is in two parts: it is prudent to ask first whether our results actually tell us something about the ocean? And second, what are the results? Though it is hard to separate the two completely, the first question is dealt with first.

1) COMPARISON BETWEEN MODEL AND OCEAN

In comparing model calculations with sea level at Bermuda, Sturges and Hong (1995) found that the model sea level results are remarkably in agreement with tide gauge observations in midocean, lending strong support to the notion that the variability in Figs. 5a,b contain information about the ocean. The model's sea level signal agreed quite well with the tide gauge observations over swings of approximately 18 cm peak to peak, with a very good match in phase and a misfit of a few centimeters or less in amplitude.

We have compared the results of Fig. 5b with the dynamic heights computed from the available hydrographic data at several locations. As is immediately obvious, the archives of open-ocean hydrographic data are suitable for comparison with time series only in exceptional cases. In order to make rigorous comparisons between model and ocean at these frequencies, it is necessary to have enough ocean data to be able to suppress the higher frequency eddy signals. Because these have large amplitudes, a sparse dataset is likely to let a considerable amount of eddy noise leak through and compromise the comparison. However, we have constructed scatterplots of our results against the available data, which show that the agreement is generally quite favorable, despite the unavoidable background of eddy noise. While this agreement is not a *strong* test, it suggests that the model results are *consistent* with observations at latitudes other than at Bermuda.

In order to tell where the model can sensibly be compared with observations, Fig. 6 shows the maximum absolute amplitude of the ocean's response. The amplitudes increase markedly from east to west with peaks near approximately 60°–70°W. The sections shown in Fig. 5, of course, were chosen to coincide with the regions of large amplitudes along 34° and 18°N.

Figure 7 shows examples of the variability in observed ocean temperature structure during two times of large fluctuations in model output. From the map for 18°N, Fig. 5b, we selected the two later time spans that have large signals: 1972–75 and 1985–86. (Although the signal near 1957 is also large, the oceanic data that we could find are too skimpy to provide a robust comparison.) Fig. 7 shows all the data in those two broad areas of space and time, in an attempt to accumulate a large enough sample of hydrographic data. In a band only 2° north–south, centered on 18°N, we use all the available data. The figure shows two clusters of data: one centered on the time of low sea level in the model and the other when sea level was high. For each hydrostation, we extracted the equivalent data point from the model, using the response of the first and the second modes. The line in Fig. 7 has a slope of 1; the scatter of the data points about the line is well within the range of the expected higher-frequency signals in the ocean. We conclude that the model output is (as at Bermuda) surprisingly consistent with the available data.

These variations are similar to those described by Joyce and Robbins (1996), who used the much richer dataset at Bermuda (32°N). They found that the temperature fluctuations reached a maximum in essentially the same depth range as in Fig. 7 and with similar variance. They also showed that the fluctuations in the main thermocline are correlated with those in the depth range 1000–1500 m. The temperature and salinity variations in the main thermocline are highly correlated. The variability below 1500 m, however, was not correlated with that in the middle of the thermocline; whether the cause is a poorer signal to noise ratio is not clear. Certainly any variations in temperature or in salinity caused by climatic fluctuations in stored heat or salt content, or the observed long-term trends, would not be reproduced in our wind-forced model.

2) OCEAN RESULTS

Some high and low departures appear as propagating wavelike features, such as the contours in both Figs. 5a and 5b that extend across the ocean in the early 1960s and the early 1980s. Others, however, appear to grow in place, such as the isolated high and low maxima. A collection of selected snapshots of the sea surface departure and a "movie" of the whole set can be found on our Web site at http://atlantic.ocean.fsu.edu.

Figures 5c and 5d show the wind curl forcing. There is little hint of any westward propagation in the wind forcing. The large positive departure in the early 1970s on the 18°N map coincides with the persistent region of forcing, but any features that appear to propagate in the ocean clearly do so because of the propagation of Rossby waves (in the ocean) rather than from any direct effects of winds propagating to the west.

In Fig. 6 there is a substantial amount of north–south structure as well as significant signals in the east–west direction. We can be certain that such structure is caused here by wind forcing because that is the only source of forcing in our model. Any hydrographic sections taken during these (or similar) times can therefore be corrected (in principle) for these wind effects in order to attempt to recover the underlying ocean circulation at lower frequencies.

Figure 8 shows two snapshots selected for the times of the maxima of Fig. 6. Figure 8a (upper) is centered on the time of the 12 cm low along 18°N, and Fig. 8b is centered on the time of the 8 cm high near Bermuda. In both cases the signal is large only in the west; a surprising wealth of detail can be found in the north–south direction.

Figure 9 compares a time series of these signals at two latitudes along 70°W. It is strikingly clear that the southern part of the gyre is anomalously low during the first half of this interval and high during the last half, whereas the northern part of the gyre has nearly the opposite phase. The suggestion from Fig. 7 is unmistakable: the above-thermocline transport in the gyre was unusually strong during the 1955–70 interval and has the sign suggesting an increased transport being fed into the Gulf Stream. Conversely, this flow then became weaker until the late 1980s. These are the features that were first called to light by the interesting results of Levitus (1990).

3) OBSERVED SPEED OF ROSSBY WAVES

Several papers have appeared recently in which the open ocean waves travel faster than the free modes would suggest, including Chelton and Schlax (1996) and others. As discussed above, in our description of computed wave speeds we pointed out that we do not find anomalously fast propagation in our results. It is well known (see White 1977) that in a simple model based on Eq. (1) with spatially uniform but time-dependent wind forcing, such as

$$\mathrm{curl}(\tau/\rho f) = a\cos(\omega t), \quad (3)$$

that the solution is the sum of a forced wave, uniform in x, and a traveling free wave that has zero amplitude at the eastern boundary; the two waves combine to give the form

$$p = \frac{2a}{\omega}\sin\left(\frac{-\omega x}{2\gamma}\right)\cos\left(\omega t + \frac{\omega x}{2\gamma}\right), \quad (4)$$

where, from (1), γ is the speed of the free waves; so the resulting wave speed, if the wind has no east–west structure, will be 2γ, twice the free wave speed. The sine term is the amplitude that grows from the eastern boundary and, perhaps surprisingly, reaches its maximum at the western side of the Atlantic for periods of approximately 100–120 months. The speed doubling does not seem to be in effect here in our results and we wonder why not.

An essential physical requirement for the doubling of the apparent wave speed as in (4) is that the curl forcing must remain coherent over the full width of the ocean. In regions of the ocean where the annual forcing is strong, the curl is at least partially coherent over the whole width of the ocean. After all, it is summer (or winter) at all longitudes, even if the details vary. Thus, a substantial degree of wind curl forcing can remain *at periods near annual* that is coherent across the ocean as these waves propagate across.

In a brief series of experiments we forced our model with simple forcing [as in (3)] with a period of 120 months and find, as shown in Fig. 10a, the simple wave response one expects, which travels at twice the model's free wave speed. The maximum in response is near the western side of the ocean. However, when random noise is added to the forcing, this result no longer holds. When the random forcing is the same order as the cosine wave, the simple, fast response is still observed; when the noise level is an order of magnitude larger, the observed response (in our model) begins to look very much like the results from COADS wind forcing, with a general westward propagation of features but otherwise erratic behavior. Figure 10b shows several examples of such results in which the noise level is a factor of 20 times the simple cosine wave. The primary forcing here (the Comprehensive Ocean–Atmosphere Data Set) is at periods of *many years.* The behavior of the wind forcing over the ocean at periods longer than 100 months obviously is much more like noise than like a pure cosine wave that is coherent over the ocean; by the time a forced wave has traveled across the ocean, several *years*have elapsed, and the wind curl is uncoupled from its previous behavior. We suggest that, in the results cited by Chelton et al. and others, the curl's coherence over the width of the ocean, near the annual period, is a major reason for these observations.

After our work was submitted for publication, we learned of the (then unpublished) results of Qiu et al. (1997). Their work focuses on a different approach to this question. They introduce eddy dissipation (rather than noise, as here) and dissipative decay of the westward propagating signals. At periods near annual or for only a few years, and at propagation distances much longer than one wavelength, their results would differ substantially from ours. The periods of concern in our work are longer; together with the smaller width of the Atlantic (than the Pacific, in their study), the longer periods here lead to the result that the decadal-scale waves in the Atlantic reach the U.S. East Coast in a distance that is small compared with the decay scale. Our results here, therefore, are consistent with theirs.

3. Discussion

We have found that wind-forced sea level variability in the open ocean at decadal timescales has peak-to-peak amplitudes of approximately 20 cm in our model; because our previous comparisons at Bermuda showed good agreement with observations, we tend to believe that the model output tells us something about the ocean. Nevertheless, the comparisons here with hydrographic data near 18°N show only that the model output is consistent with the data and do not allow a strong test. These decadal signals are as large as the higher-frequency"eddy signals" and are accompanied by departures of the main thermocline that have a first vertical-mode-like structure. These large signals can seriously frustrate attempts to deduce the lower-frequency circulation of the ocean by methods that treat historical hydrographic data as a synoptic dataset. There is the possibility, however, that historical data can be corrected for these effects to allow such calculations to be performed with much higher reliability.

The signals in our model are completely wind forced. At the latitude of the subtropical gyres, the *annual cycles*of stored heat are large but are not contained in our low-frequency model. Based on the comparisons at Bermuda (Sturges and Hong 1995, and others), it appears that the wind-forced fluctuations recover essentially all the variability. There are few degrees of freedom, to be sure, but (at our present level of accuracy) in this frequency band, and at these latitudes, there is no residual signal to be explained by atmospheric buoyancy effects. This is a surprising result.

What happens to these signals when they reach the Gulf Stream or the western wall? One conclusion from the results of Greatbatch et al. (1991) is that the increased flow to the west is absorbed into the transport of the Gulf Stream. Thus, the transport associated with the north–south slope of the sea surface in Figs. 8 and 9, one assumes, is to a large extent diverted into the Gulf Stream. Order-of-magnitude estimates show that these effects may potentially have magnitudes as large as those observed at the coast. Our studies of these changes will be reported in a following paper.

Acknowledgments

We thank Dr. Steve Gill of the National Ocean Service, NOAA, for a great deal of help with obtaining tide-gauge data. Robert Gelfeld and Sydney Levitus were most helpful in supplying hydrographic data from the National Oceanographic Data Center. We thank Bo Qiu for giving us a copy of his work prior to publication. We also would like to acknowledge many helpful conversations with Prof. William Dewar, and constructive comments on the manuscript by Dr. K. Brink and two anonymous but helpful reviewers. This work was supported by the National Oceanic and Atmospheric Administration under Grant NA27GP0343 and by the F.S.U. Center for the Study of Sea Level Change. During the final revision of the manuscript the first author was supported by NSF.

REFERENCES

Barnett, T. P., 1984: The estimation of “global” sea level change: A problem of uniqueness. *J. Geophys. Res.,* **89** (C5), 7980–7988..

Chang, P., and S. G. H. Philander, 1989: Rossby wave packets in baroclinic mean currents. *Deep-Sea Res.,* **36,** 17–37..

Chelton, D. B., and M. G. Schlax, 1996: Global observations of oceanic Rossby waves. *Science,* **272,** 234–238..

Douglas, B. C., 1992: Global sea level acceleration. *J. Geophys. Res.,***97** (C8), 12699–12706..

Ezer, T., G. L. Mellor, and R. J. Greatbatch, 1995: On the interpentadal variability of the North Atlantic Ocean: Model simulated changes in transport, meridional heat flux and coastal sea level between 1955–1959 and 1970–1974. *J. Geophys. Res.,* **100** (C6), 10559–10566..

Greatbatch, R. J., A. F. Fanning, A. D. Goulding, and S. Levitus, 1991: A diagnosis of interpentadal circulation changes in the North Atlantic. *J. Geophys. Res.,* **96** (C4), 22009–22023..

Hicks, S. D., H. A. Debaugh, and L. E. Hickman, 1983: Sea level variations for the United States 1855–1980, Tech. Rep., NOAA, NOS, Silver Spring, MD, 170 pp. [Available from NOAA, National Ocean Service, 1315 East–West Highway, Silver Spring, MD 20910.].

Joyce, T. M., and P. Robbins, 1996: The long-term hydrographic record at Bermuda. *J. Climate,* **9,** 3121–3131.. Find this article online

Kessler, W. S., 1990: Observations of long Rossby waves in the northern tropical Pacific. *J. Geophys. Res.,* **95** (C4), 5183–5217..

Krauss, W., and C. Wuebber, 1982: Response of the North Atlantic to annual wind variations along the eastern coast. *Deep-Sea Res.,***29,** 851–868..

Levitus, S., 1990: Interpentadal variability of steric sea level and geopotential thickness of the North Atlantic Ocean, 1970–1974 versus 1955–1959. *J. Geophys. Res.,* **95** (C4), 5233–5238..

Liu, Z., 1993: Thermocline forced by varying Ekman pumping. Part II: annual and decadal Ekman pumping. *J. Phys. Oceanogr.,* **23,**2523–2540..

Maul, G. A., and K. Hanson, 1991: Interannual coherence between North Atlantic atmospheric surface pressure and composite southern USA sea level. *Geophys. Res. Lett.,* **18,** 653–656..

Mayer, D. A., and R. H. Weisberg, 1993: A description of COADS surface meteorological fields and the implied Sverdrup transports for the Atlantic Ocean from 30° S to 60° N. *J. Phys. Oceanogr.,***23,** 2201–2221..

Meyers, G., 1979: On the annual Rossby wave in the tropical North Pacific Ocean. *J. Phys. Oceanogr.,* **9,** 663–674..

Picaut, J., and L. Sombardier, 1993: Influence of density stratification and bottom depth on vertical mode structure functions in the tropical Pacific. *J. Geophys. Res.,* **98** (C8), 14727–14737..

Price, J. M., and L. Magaard, 1986: Interannual baroclinic Rossby waves in the midlatitude North Atlantic. *J. Phys. Oceanogr.,* **16,**2061–2070..

Qui, B., W. Miao, and P. Müller, 1997: Propagation and decay of forced and free baroclinic Rossby waves in off-equatorial oceans. *J. Phys. Oceanogr.,* **27,** 2405–2417..

Slutz, R. J., S. D. Woodruff, R. L. Jenne, and P. M. Steurer, 1985: A Comprehensive Ocean–Atmosphere Data Set. *Bull. Amer. Meteor. Soc.,* **66,** 1239–1250.. Find this article online

Sturges, W., and B. G. Hong, 1995: Wind forcing of the Atlantic thermocline along 32° N at low frequencies. *J. Phys. Oceanogr.,***25,** 1706–1715..

White, W. B., 1977: Annual forcing of baroclinic long waves in the tropical North Pacific Ocean. *J. Phys. Oceanogr.,* **7,** 50–61..

Woodworth, P. L., 1990: A search for accelerations in records of European mean sea level. *Int. J. Climatol.,* **10,** 129–143..

Wunsch, C., 1992: Decade-to-century changes in the ocean circulation. *Oceanography,* **5** (2), 99–106..

Figures

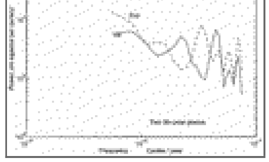

Click on thumbnail for full-sized image.

Fig. 1. The spectrum of sea level at low frequencies: Charleston, South Carolina, based on 57 years of data; only periods longer than a year are shown here. The two curves show the results from the first 30 years versus the last 30 years of data. Each calculation uses a full cosine bell data window to reduce leakage and then is smoothed (in frequency) by a single pass of a Hanning filter to preserve the signal at the lowest frequencies.

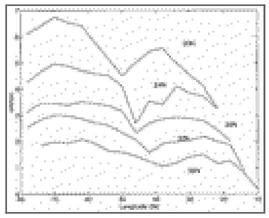

Click on thumbnail for full-sized image.

Fig. 2. Speeds of the long Rossby waves in the model. Only every other latitude band used is shown. The speeds were computed for the first vertical mode based on the data available from NODC in each 4° by 4° box (see text).

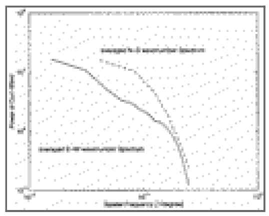

Click on thumbnail for full-sized image.

Fig. 3. Average wavenumber spectra of wind curl forcing based on COADS data. The east–west spectrum is averaged from 18° to 42°N across the width of the Atlantic. The calculation uses 2° resolution, but the wind stress was initially integrated around 4° boxes to compute the curl. For simplicity in plotting the east–west variability, the power is shown as if each degree of longitude were 100 km in length.

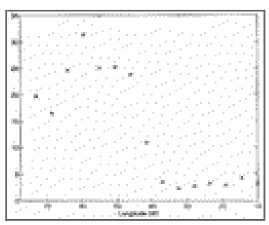

Click on thumbnail for full-sized image.

Fig. 4. Relative power in the north–south wavenumber spectrum of wind curl from COADS data (from Fig. 2); the mean of the two lowest wavenumbers is shown.

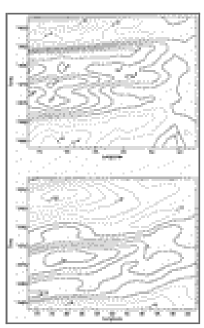

Click on thumbnail for full-sized image.

Fig. 5a,b. Computed fluctuations in the height of sea level across the Atlantic at 34°N (upper) and 18°N (lower) as a function of longitude and time. Heights are in centimeters.

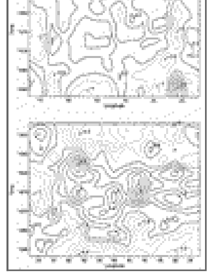

Click on thumbnail for full-sized image.

Fig. 5c,d. Computed fluctuations in the Ekman pumping across the Atlantic at 34°N (upper) and 18°N (lower), as a function of longitude and time, that are used to force the results shown in Figs. 5a,b.

Click on thumbnail for full-sized image.

Fig. 6. The maximum *absolute* amplitude of the ocean’s response in the model; amplitudes are in centimeters.

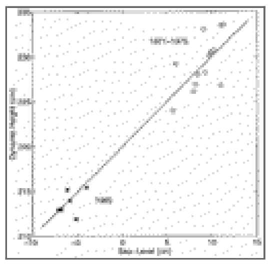

Click on thumbnail for full-sized image.

Fig. 7. Comparison between model output and dynamic height, 100–1000 db, from all hydrographic data during time intervals of large departures (as determined from Fig. 5b), using the times and positions of the available data to extract model output.

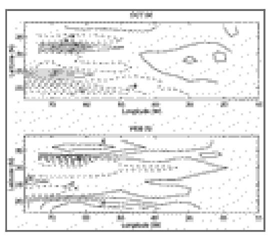

Click on thumbnail for full-sized image.

Fig. 8. Maps of model sea surface departures for the times of the maxima near 75°W in Fig. 6: (a), upper, is centered on the time of the 12 cm low along 18°N and (b), lower, is centered on the 8 cm high near Bermuda. Negative departures are dashed; heights are in centimeters.

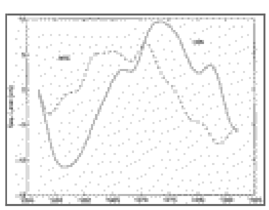

Click on thumbnail for full-sized image.

Fig. 9. Departures of model sea level along 70°W for two latitudes: 18°N (solid curve) and 36°N (dashed). Time is in years.

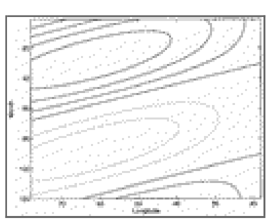

Click on thumbnail for full-sized image.

Fig. 10a. Model output for a test case; forcing is by a single cosine wave, uniform in *x*, a period of 120 months, with wave speed set at a constant 3 cm s^{-1}. The apparent propagation is twice the free wave speed, and there is a maximum in the western ocean. See text.

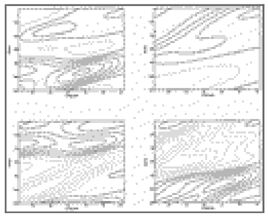

Click on thumbnail for full-sized image.

Fig. 10b–e. Examples of model output for a test case, as in Fig. 10a except that random noise has been added to the forcing. The noise amplitude is a factor of 20 times that of the cosine wave. Solid contours represent positive sea surface displacement; amplitudes are arbitrary. The speed doubling is no longer apparent.

Corresponding author address: Dr. W. Sturges, Department of Oceanography, The Florida State University, Tallahassee, FL 32306-4320.

E-mail: sturges@ocean.fsu.edu

[1] The tide gauge data used in this work are available via anonymous ftp from atlantic.ocean.fsu.edu.